Longitudinal dynamics for mesons on the light cone

Yang Li[1] and James P. Vary[2]

[1]*Department of Modern Physics, University of Science and Technology of China, Hefei, Anhui 230026, China*

[2]*Department of Physics and Astronomy, Iowa State University, Ames, Iowa 50011, USA*

(Received 25 February 2022; accepted 20 May 2022; published 7 June 2022)

We survey a set of proposed light-front models for confinement in the valence quark sector of the mesons and portray similarities as well as differences. We present the spectroscopies for the light mesons that result from a selection of longitudinal confinement forms. We note that the Sturm-Liouville theory provides a unifying framework for many elements of this comparison.

DOI: 10.1103/PhysRevD.105.114006

I. INTRODUCTION

The light-front Schrödinger wave equation (LFSWE) provides a relativistic semiclassical first approximation to QCD for mesons represented as quark and antiquark bound states [1],

$$\left[\frac{\vec{k}_\perp^2 + m_q^2}{x} + \frac{\vec{k}_\perp^2 + m_{\bar{q}}^2}{1-x} + V\right]\psi(x, \vec{k}_\perp) = M^2\psi(x, \vec{k}_\perp). \quad (1)$$

Here, the effective potential V encodes the nonperturbative dynamics of QCD at low-energy resolution. Remarkably, Brodsky and de Tramond discovered that the LFSWE in the chiral limit ($m_q = m_{\bar{q}} = 0$) can be identified with the equation of motion of strings in the fifth dimension of anti–de Sitter (AdS) space thus establishing an extraordinary connection between light-front QCD and AdS/QCD, a bottom-up approach known as light-front holography (LFH) [2]. LFH has been successfully applied to describing the hadron spectroscopy, including the spectra of mesons [2–6], the infrared behavior of the strong coupling [7], hadron form factors [2,8–10] and parton distributions [11,12]. An excellent review of this approach is found in Ref. [13].

Light-front holography addresses the chiral limit where only the dynamics of the transverse degrees of freedom (d.o.f.) are considered. Recently, attention has focused on the role of longitudinal dynamics [14–24]. The longitudinal dynamics is important for incorporating finite quark masses, chiral dynamics and longitudinal excitations as well as for identifying the physical states in the excitation spectrum [25]. Unlike the transverse d.o.f., the longitudinal dynamics in the presence of transverse dynamics of the LFSWE has not been posed from underlying principles.

In light of various proposals in the literature, it is tempting to compare these longitudinal confining interactions. Ahmady *et al.* compared the hadron spectra employing the 't Hooft model and our model [20]. Shuryak and Zahed compared the effective light-front Hamiltonian obtained from the Nambu-Goto string having massive ends with a phenomenological model we (with others) introduced [22]. Weller and Miller further compared the longitudinal confining potentials of these three models and the corresponding wave functions [26]. In this work, we discuss the role of longitudinal dynamics in LFSWE. In particular, we focus on the endpoint behavior of the wave functions and the scaling of the eigenvalues. We show that this behavior is closely related to the singularities of the corresponding LFSWE. This observation enables us to consider a broader class of longitudinal confining potentials based on the Sturm-Liouville (SL) theory. We present several concrete examples.

This perspective is consistent with the traditional quantum many-body approach to self-bound systems, e.g., atoms, molecules, and nuclei. There, first approximations are employed to chart out a set of "orbits" or "shells" of the system. Then, the wave functions of these orbits are adopted as the basis within which the full Hamiltonian operator is diagonalized to obtain the "exact" results. In light of this link to the quantum many-body treatment, basis light-front quantization (BLFQ) [27], we referred to our recent LFSWE approach for light mesons as BLFQ_0. In the heavy quark systems, the nonrelativistic potential model is a valid first approximation [28]. This model is augmented to the Hamiltonian QCD in Coulomb gauge to address the full QCD dynamics [29] (see Ref. [30] for a recent review). In the light hadron sector, light-front holography plays an analogous role with its remarkable phenomenological successes. Recently, it was argued that the endpoint

asymptotics of the longitudinal dynamics are essential for implementing the Gell-Mann-Oakes-Renner (GMOR) relation—a direct consequence of chiral symmetry breaking in the light sector [18,25].

The reminder of this work is organized as follows. Section II introduces the LFSWE within the separation of variables ansatz and its application in QCD, the light-front holographic QCD. We then discuss the need for a longitudinal dynamics and compare various proposals from the literature in Sec. III. In the next section, Sec. IV, we construct a general class of longitudinal potentials based on the Sturm-Liouville theory. Several specific cases are investigated. Finally, we conclude in Sec. V.

II. FORMALISM

Formally, the LFSWE is a low-energy effective theory of QCD. Therefore, it may be obtained from a Hamiltonian renormalization group evolution, either the Okubo-Suzuki-Lee type [31–36] or the flow-equation type [37–39]. Alternatively, it can be viewed as the truncation up to the valence Fock sector; hence, the Tamm-Dancoff type of approximation is applied [40,41]. These formal connections to QCD make it possible to systematically improve the LFSWE, as shown in Refs. [42–45]. In either approach, one can write down the wave equation,

$$\left[\frac{\vec{k}_\perp^2+m_q^2+\Sigma_s(x,\vec{k}_\perp)}{x}+\frac{\vec{k}_\perp^2+m_{\bar{q}}^2+\Sigma_{\bar{s}}(1-x,-\vec{k}_\perp)}{1-x}\right]\psi_{s\bar{s}/h}^{(J,m_J)}(x,\vec{k}_\perp)$$
$$+\sum_{s',\bar{s}'}\int\frac{\mathrm{d}x'}{2x'(1-x')}\int\frac{\mathrm{d}^2k'_\perp}{(2\pi)^3}V_{s\bar{s}s'\bar{s}'}(x,\vec{k}_\perp,x',\vec{k}'_\perp)\psi_{s'\bar{s}'/h}^{(J,m_J)}(x',\vec{k}'_\perp)=M_h^2\psi_{s\bar{s}/h}^{(J,m_J)}(x,\vec{k}_\perp). \tag{2}$$

Σ_σ is the quark self-energy and needs to be solved from the gap equation. In the first approximation, we can absorb the self-energy in an effective quark mass. J is the total angular momentum and m_J is its magnetic projection. ψ is the wave function which is normalized according to

$$\sum_{s\bar{s}}\int_0^1\frac{\mathrm{d}x}{2x(1-x)}\int\frac{\mathrm{d}^2k_\perp}{(2\pi)^3}\bar{\psi}_{s\bar{s}/h}^{(Jm_J)}(x,\vec{k}_\perp)\psi_{s\bar{s}/h'}^{(J'm'_J)}(x,\vec{k}_\perp)$$
$$=\delta_{hh'}\delta_{m_J,m'_J}. \tag{3}$$

Subscript h indicates the hadron species. This wave equation corresponds to the effective Hamiltonian $H_{\mathrm{eff}}=(\vec{k}_\perp^2+m_q^2)/x+(\vec{k}_\perp^2+m_{\bar{q}}^2)/(1-x)+V$. The normalization adopted here stems from the Lorentz invariant phase space element,

$$\int\frac{\mathrm{d}^4p}{(2\pi)^4}2\pi\delta(p^2-m^2)=\int\frac{\mathrm{d}^3p}{(2\pi)^3 2p^0}\theta(p^0)$$
$$=\int\frac{\mathrm{d}p^+\mathrm{d}^2p_\perp}{(2\pi)^3 2p^+}\theta(p^+). \tag{4}$$

To associate the eigenvalues and eigenfunctions to hadrons, we need to compute the discrete symmetries P and C. They are represented as [46]

$$C=\int_0^1\frac{\mathrm{d}x}{2x(1-x)}\int\frac{\mathrm{d}^2k_\perp}{(2\pi)^3}\psi^*_{s\bar{s}}(x,\vec{k}_\perp)\psi_{\bar{s}s}(1-x,-\vec{k}_\perp), \tag{5}$$

$$(-1)^JP=\int_0^1\frac{\mathrm{d}x}{2x(1-x)}\int\frac{\mathrm{d}^2k_\perp}{(2\pi)^3}\psi^*_{s\bar{s}}(x,\vec{k}_\perp)\psi_{-s-\bar{s}}(x,\tilde{k}_\perp), \tag{6}$$

where $\tilde{k}_\perp=(-k_x,k_y)$. The mirror parity $(-1)^JP$ is employed here since it is a more convenient observable on the light front [46]. Since the mirror parity flips the sign of the spin, we can use the $m_J=0$ state to compute the mirror parity.

A. Separation of variables

In the massless limit, the kinetic energy becomes $\vec{k}_\perp^2/x(1-x)$, which depends only on a 2D variable $\vec{\kappa}_\perp\equiv\vec{k}_\perp/\sqrt{x(1-x)}$. It is natural to assume the system in the chiral limit also depends only on $\vec{\kappa}_\perp$ and its conjugate coordinate $\vec{\zeta}_\perp=i\nabla_{\kappa_\perp}=\sqrt{x(1-x)}\vec{r}_\perp$ [2]. In the more general case, especially when the quark masses are not zero, we can assume that the interaction is separable; $V=V_\perp+V_\parallel$, an ansatz first explicitly introduced by Chabysheva and Hiller [14] (cf. Ref. [9]). We note that the separation of the transverse and longitudinal dynamics is natural in light-front QCD [47]. Figure 1 shows two representative light-front QCD interactions. Figure 1(a) involves the exchange of the purely transverse gluons while Fig. 1(b) involves the instantaneous interaction in the

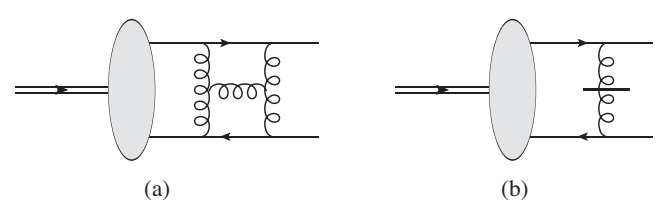

FIG. 1. Representative light-front QCD interactions contributed to the (a) transverse and (b) longitudinal effective interactions, respectively.

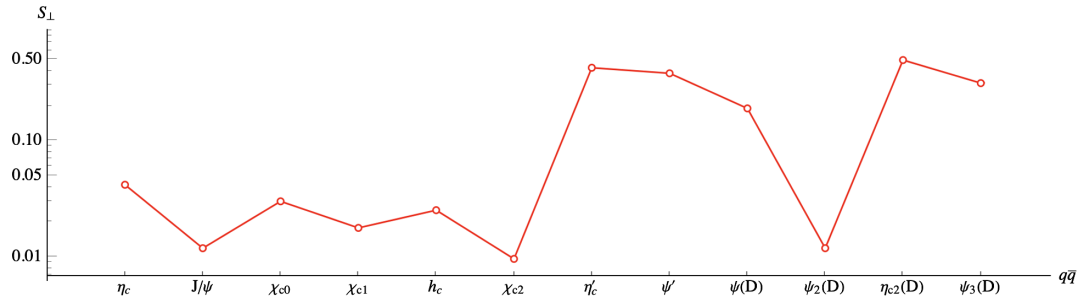

FIG. 2. Entanglement entropy between the transverse and the longitudinal d.o.f. for charmonium states obtained from BLFQ. The effective Hamiltonian adopts a separable confining (holographic confinement plus the LMZV longitudinal confinement) along with a nonseparable one-gluon-exchange interaction [52].

longitudinal direction. The latter survives in $1+1$D as the Schwinger-'t Hooft type of interaction [48–50].

Of course, the true effective interaction between a quark and an antiquark may not be separable; for instance, the one-gluon-exchange interaction. A proper metric of the separability is the entanglement entropy $S_\perp$ between the transverse and the longitudinal d.o.f., which is defined as the von Neumann entropy for the reduced density matrix, $S_\perp = -\mathrm{tr}[\rho_\perp \log \rho_\perp]$ [51]. Figure 2 shows the entanglement entropy between the transverse and the longitudinal d.o.f. for charmonium states obtained from a nonseparable interaction [52]. The effective Hamiltonian adopts a separable confining interaction (holographic confinement plus the Li-Maris-Zhao-Vary (LMZV) longitudinal confinement) along with a nonseparable one-gluon-exchange interaction. As one can see, $S_\perp$ is generally small for the ground states—indicating that these states are physically separable within this model. In this work, we adopt the separation of variable ansatz, which should provide a good description for the low-lying states.

With this ansatz, the mass eigenvalues $M^2 = M_\perp^2 + M_\parallel^2$ and the wave function are also separable,

$$\psi(x, \vec{k}_\perp) = \sqrt{4\pi}\phi(\vec{k}_\perp/\sqrt{x(1-x)})\chi(x). \tag{7}$$

We obtain two LFSWEs [14],

$$[\vec{\kappa}_\perp^2 + V(\vec{\zeta}_\perp)]\phi(\vec{\kappa}_\perp) = M_\perp^2\phi(\vec{\kappa}_\perp), \tag{8}$$

$$\left[\frac{m_q^2}{x} + \frac{m_{\bar{q}}^2}{1-x} + V_\parallel(\tilde{z})\right]\chi(x) = M_\parallel^2\chi(x). \tag{9}$$

Here, the longitudinal effective potential $V_\parallel$ depends on the boost invariant longitudinal coordinate $\tilde{z} = \frac{1}{2}p^+x^-$ [or other related longitudinal coordinate variables, e.g., (24)], introduced by Miller and Brodsky [53]. We note that even in the massless limit, Eq. (9) is still required to have nontrivial solutions. Hereafter, we consider specific spin configurations (the leading-twist spin components) and the explicit spin indices will be suppressed, except for the purpose of state identification. Note that the separation of variables ansatz requires that the variables $\vec{\zeta}_\perp$ and $\tilde{z}$ (or other related longitudinal coordinate variables) are independent. Since $\vec{\zeta}_\perp = \sqrt{x(1-x)}\vec{r}_\perp$ depends on x, $\tilde{z}$ should be defined as a differential operator against $\vec{\zeta}_\perp$, viz. $\tilde{z} = i\frac{\partial}{\partial x}|_{\vec{\zeta}_\perp}$.

It is convenient to normalize the transverse and longitudinal wave functions,

$$\int \frac{\mathrm{d}^2\kappa_\perp}{(2\pi)^2}|\phi(\vec{\kappa}_\perp)|^2 = 1, \qquad \int_0^1 \mathrm{d}x|\chi(x)|^2 = 1. \tag{10}$$

It is also useful to introduce a longitudinal wave function $X(x) = \sqrt{x(1-x)}\chi(x)$ with the normalization,

$$\int_0^1 \frac{\mathrm{d}x}{x(1-x)}|X(x)|^2 = 1. \tag{11}$$

In our convention, $X(x)$ is proportional to the distribution amplitude. This is related to the alternative normalization convention of the wave function $\tilde{\Psi}(x, \vec{\zeta}_\perp)$ or its transverse Fourier conjugate,

$$\begin{aligned}\Psi(x, \vec{\kappa}_\perp) &= \int \frac{\mathrm{d}^2\kappa_\perp}{(2\pi)^2}\tilde{\Psi}(x, \vec{\zeta}_\perp)e^{-i\vec{\kappa}_\perp\cdot\vec{\zeta}_\perp} \\ &= \psi(x, \vec{k}_\perp)/\sqrt{x(1-x)}.\end{aligned} \tag{12}$$

Under this convention, the normalizations of the wave functions are [recall $\vec{\kappa}_\perp = \vec{k}_\perp/\sqrt{x(1-x)}$, $\vec{\zeta}_\perp = \sqrt{x(1-x)}\vec{r}_\perp$],

$$\begin{aligned}&\int_0^1 \mathrm{d}x \int \frac{\mathrm{d}^2k_\perp}{16\pi^3}|\Psi(x, \vec{k}_\perp/\sqrt{x(1-x)})|^2 = 1, \\ &\frac{1}{4\pi}\int_0^1 \frac{\mathrm{d}x}{x(1-x)}\int \mathrm{d}^2\zeta_\perp|\tilde{\Psi}(x, \vec{r}_\perp)|^2 = 1.\end{aligned} \tag{13}$$

With this convention, the separable wave function takes the form, $\tilde{\Psi}(x,\vec{\zeta}_\perp) = \sqrt{4\pi}\tilde{\phi}(\zeta_\perp)X(x)$, where $\tilde{\phi}$ is the Fourier transform of ϕ,

$$\tilde{\phi}(\zeta_\perp) = \int \frac{d^2\kappa_\perp}{(2\pi)^2} e^{i\vec{\kappa}_\perp\cdot\vec{\zeta}_\perp}\phi(\vec{\kappa}_\perp). \tag{14}$$

As an example, the pion wave function in LFH in the massless limit is $\chi(x) = 1$ and $X(x) = \sqrt{x(1-x)}$.

B. Light-front holography

In LFH, the transverse effective potential is determined by the dilaton profile $\Phi(z)$ in AdS/QCD, $V_\perp = (1/2)\Phi'' + (1/4)\Phi'^2 + [(2J-3)/2z]\Phi'$ [54]. For the soft-wall profile, $V_\perp = \kappa^4\zeta_\perp^2 + 2\kappa^2(J-1)$. Here, κ is the strength of the confinement in mass dimension. J is the total angular momentum. The parton transverse separation $\zeta_\perp = \sqrt{x(1-x)}r_\perp$ is mapped to the fifth coordinate z in anti–de Sitter space. The mass eigenvalues are

$$M_{nmJ}^2 = 4\kappa^2\left(n + \frac{J+|m|}{2}\right). \tag{15}$$

where n, and m are the radial and angular quantum numbers in the transverse plane ($\vec{\zeta}_\perp$). The corresponding wave functions are 2D harmonic oscillator functions,

$$\phi_{nm}(\vec{\zeta}_\perp) = \kappa\sqrt{\frac{n!}{\pi(n+|m|)!}}e^{-\frac{\kappa^2\zeta_\perp^2}{2}}(\kappa\zeta_\perp)^{|m|}L_n^{|m|}(\kappa^2\zeta_\perp^2)e^{im\arg\vec{\zeta}_\perp}, \tag{16}$$

where n and m are the transverse radial and angular quantum numbers. The ground state $n = 0$, $m = 0$, and $J = 0$ describes the pion, whose mass is predicted to vanish. Its wave function is Gaussian,

$$\psi_\pi(x,\vec{k}_\perp) = \frac{4\pi}{\kappa}\exp\left[-\frac{\vec{k}_\perp^2}{2\kappa^2 x(1-x)}\right]. \tag{17}$$

To incorporate the finite quark masses, Brodsky and de Téramond employed a longitudinal wave function without explicitly introducing the longitudinal dynamics [9]. This ansatz, known as the invariant mass ansatz (IMA), is based on the observation that with the presence of finite quark mass, the light-front kinetic energy becomes

$$\frac{\vec{k}_\perp^2}{x(1-x)} \to \frac{\vec{k}_\perp^2 + m_q^2}{x} + \frac{\vec{k}_\perp^2 + m_{\bar{q}}^2}{1-x}. \tag{18}$$

Hence, it is instructive to make the substitution in the wave functions. Then the pion wave function becomes

$$\psi_\pi(x,\vec{k}_\perp) = N\frac{4\pi}{\kappa}\exp\left[-\frac{\vec{k}_\perp^2 + m_q^2}{2\kappa^2 x(1-x)}\right]. \tag{19}$$

N is a normalization constant. In other words, the longitudinal wave function becomes

$$\chi_{\rm IMA}(x) = N\exp\left[-\frac{m_q^2}{2\kappa^2 x(1-x)}\right]. \tag{20}$$

The pion mass is also shifted to a nonzero value by

$$M_\pi^2 = \int_0^1 \frac{dx}{2x(1-x)}\int\frac{d^2k_\perp}{(2\pi)^3}|\psi_\pi(x,\vec{k}_\perp)|^2\frac{m_q^2}{x(1-x)}. \tag{21}$$

In the vicinity of the chiral limit, the theory predicts a near quadratic quark-mass dependence of the pion mass, $M_\pi^2 \approx 2m_q^2(\ln\kappa^2/m_q^2 - \gamma_{\rm E})$, where $\gamma_{\rm E} \approx 0.577216$ is Euler's constant [18]. The scaling of the pion mass M_π as a function of the quark mass m_q is inconsistent with the results from chiral symmetry breaking, which predicts a linear dependence instead, a result also known as the Gell-Mann-Oakes-Renner (GMOR) relation [55],

$$f_\pi^2 M_\pi^2 = 2m_q\langle 0|\bar{q}q|0\rangle + O(m_q^2). \tag{22}$$

Gutsche *et al.* suggested replacing the longitudinal wave function (20) from IMA by a power-lawlike function to generate the GMOR relation [25].

Another issue with IMA is the lack of longitudinal excitations, which leads to inconsistencies in state identification [17,18]. For example, in LFH the mass of $\rho(1D)$ is degenerate with the mass of $\rho(2S)$, and is 400 MeV lower than the mass of $\rho(1700)$, which is usually identified as $\rho(1D)$. Indeed, in LFH, $\rho(1700)$ is identified as $\rho(3S)$ instead. Similarly, $K_1(1400)$ in LFH is identified as 2^3P_1 as opposed to the conventional identification 1^1P_1. The resulting mass is higher than the experimental measurements.

For states identified with quantum numbers (n, m, S, J) in LFHQCD with IMA, $(-1)^J P = (-1)^{m+S+1}$, $C = (-1)^{m+S}$. From these relations, quantum number assignments of the scalars a_0 (0^{++}), the axial vectors b_1 (1^{+-}), and the axial tensors a_2 (2^{++}) etc., are not compatible with the discrete symmetries. The source of the discrepancy is the lack of longitudinal degrees of freedom in LFH with IMA. Indeed, in the basis function approach to the same quantum numbers, these states are excited in the longitudinal direction [52]. Indeed, Nielsen and Brodsky recently reinterpreted the scalars 0^{++} and axial vectors $1^{+\pm}$ as tetraquark states based on supersymmetric construction of light-front holography [56].

A possible alternative is to invoke the total orbital angular momentum L and to assume that the LFH wave functions with IMA are only valid for states $L_z = |m| = L$. Note that L is not a good quantum number in relativistic

quantum mechanics. The obtained wave function may not be in leading twist ($L_z = 0$), either. In contrast, incorporating the longitudinal dynamics will provide the complete set of wave functions and the assignment of P and C does not rely upon these interpretations.

III. LONGITUDINAL CONFINEMENT

The issues encountered in LFH point to the need for longitudinal dynamics. Indeed, as we mentioned, the decoupling of the transverse and longitudinal d.o.f. in Eqs. (8)–(9) does not necessarily imply the absence of the longitudinal dynamics. The presence of longitudinal confinement naturally leads to longitudinal excitations which ensure the correct state identification, similar to the nonrelativistic cases but with exact discrete quantum numbers on the light front. Now, the new set of quantum numbers becomes (n, m, l, S, J), where l counts the number of nodes in the longitudinal direction. Under charge conjugation, $x \leftrightarrow (1-x)$ generates an extra sign $(-1)^l$. Hence, the charge conjugation quantum number should become $C = (-1)^{m+l+S}$. One can see that this resolves discrepancies associated with state identification in LFHQCD for states with longitudinal excitations. For nonseparable states involving more than one eigenstate of the effective Hamiltonian, one can always go back Eqs. (5)–(6). Hence, a longitudinal confinement is required to maintain the 3D structure of hadrons.

Of course, the longitudinal dynamics is also needed to incorporate the finite quark masses dynamically. This was first done by Chabysheva and Hiller utilizing the 't Hooft model [14],

$$(V_{\mathrm{tH}} \circ \chi)(x) = \frac{g^2}{\pi} \mathrm{P} \int \mathrm{d}y \frac{\chi(x) - \chi(y)}{(x-y)^2}, \tag{23}$$

where the principle value prescription $\mathrm{P}(1/x^2) \equiv (1/2)[1/(x^2 + i\epsilon) + 1/(x^2 - i\epsilon)]$ is applied to the pole in the integrand. Chabysheva and Hiller focused on a specific solution with $m_q = g/\sqrt{\pi}$. The 't Hooft model as the longitudinal confinement was recently revisited by Ahmady *et al.* [20,21].

Another longitudinal confinement based on a construction of the harmonic oscillator potential was proposed by Głazek and Trawiński [15,16]. They introduce a third momentum $\kappa_\parallel \equiv (m_q + m_{\bar{q}})(x - \hat{m}_q)/\sqrt{x(1-x)}$, where $\hat{m}_q = m_q/(m_q + m_{\bar{q}})$. The longitudinal confining potential is defined as the harmonic oscillator potential of the conjugate coordinate $\zeta_\parallel$ of $\kappa_\parallel$, viz.

$$V_{\mathrm{GT}} = \kappa^4 \zeta_\parallel^2. \tag{24}$$

The resulting mass squared eigenvalues obey the linear Regge trajectory, $M_l^2 = \kappa^2(l + \frac{1}{2})$. The ground-state wave function is Gaussian,

$$\chi_{\mathrm{GT}}(x) = N \exp\left[-(m_q + m_{\bar{q}})^2 \frac{(x - \hat{m}_q)^2}{2\kappa^2 x(1-x)}\right] = N' \exp\left[-\frac{1}{2\kappa^2}\left(\frac{m_q^2}{x} + \frac{m_{\bar{q}}^2}{1-x}\right)\right]. \tag{25}$$

Therefore, this model can be viewed as a generalization of the IMA.

The quark masses adopted in Refs. [14–16] are of the order of the constituent quark mass (~300 MeV). In Ref. [17], Li, Maris, Zhao, and Vary proposed an analytically solvable longitudinal confining potential and applied it to the quarkonium in the framework of BLFQ. In Ref. [18], we further show that in the vicinity of the chiral limit, the LMZV model reproduces the GMOR relation as well as the signature power-law wave function. This is sometimes termed BLFQ_0 to distinguish from the applications to the heavy flavors where the longitudinal coupling σ is chosen to match to the transverse confining strength in the nonrelativistic (NR) limit. The longitudinal confinement takes the form,

$$(V_{\mathrm{LMZV}} \circ \chi)(x) = -\sigma^2 \frac{\mathrm{d}}{\mathrm{d}x}\left(x(1-x)\frac{\mathrm{d}}{\mathrm{d}x}\chi(x)\right), \tag{26}$$

where σ is the strength of the longitudinal confinement. The same longitudinal confinement is adopted by de Tramond and Brodsky in Ref. [19] to incorporate chiral symmetry breaking. Both works note the close relation between the $\mathrm{LMZV/BLFQ}_0$ model and the 't Hooft model. The latter is known to exhibit the chiral symmetry breaking via the Kosterlitz–Thouless (KT) mechanics [57]. From the ground state masses in the vicinity of the chiral limit $M_{\mathrm{LMZV}}^2 = \sigma(m_q + m_{\bar{q}}) + O(m_{q,\bar{q}}^2)$, and $M_{\mathrm{tH}}^2 = g\sqrt{\frac{\pi}{3}}(m_q + m_{\bar{q}}) + O(m_{q,\bar{q}}^2)$, we can identify $\sigma = g\sqrt{\frac{\pi}{3}} = |\langle \bar{q}q \rangle|/f_\pi^2$. The longitudinal wave function of the $\mathrm{LMZV/BLFQ}_0$ model is

$$\chi_{\mathrm{LMZV}}(x) = N x^{\alpha_1}(1-x)^{\alpha_2}, \tag{27}$$

where $\alpha_i = m_i/\sigma$. The 't Hooft wave function is

$$\chi_{\mathrm{tH}}(x) \doteq N x^{\beta_1}(1-x)^{\beta_2}. \tag{28}$$

The exponents $\beta_{1,2}$ satisfy $\pi m_i^2/g^2 = 1 - \pi\beta_i \cot \pi\beta_i$. The solution in the vicinity of the chiral limit is, $\beta_i = (m_i/g)(\sqrt{3/\pi}) = \alpha_i$, identical to those of the $\mathrm{LMZV/BLFQ}_0$ model. In other words, the ground-state mass eigenvalue and eigenfunctions of the both models are identical. These two models differ in the excited state masses. For large excitation, the mass eigenvalues of the 't Hooft model obey the linear Regge trajectory, $M_n^2 \propto n$, whereas those of the $\mathrm{LMZV/BLFQ}_0$ model are quadratic, $M_n^2 \propto n(n+1)$. A detailed comparison of the hadron spectra using the 't Hooft model and the $\mathrm{LMZV/BLFQ}_0$

model with the original predictions from LFH with IMA is reported by Ahmady *et al.* [21].

Note that Ahmady *et al.* effectively imposed a constraint $l \geq n + m$ on the hadron spectra and eliminated low-lying states without the required longitudinal excitations. For example, the scalar (0^{++}) $a_0(980)$ is identified as $(n, m, S) = (0, 1, 1)$ in LFH with IMA, with a predicted mass $M_{\mathrm{IMA}} = 0.76$ GeV. In the LMZV/BLFQ$_0$ model, this particle is identified as $(n, m, l, S) = (0, 0, 1, 1)$ with a predicted mass $M_{\mathrm{LMZV}} = 0.91$ GeV. Both models are consistent with the quark model identification 1^3P_0 while the latter improves the theoretical prediction. By contrast, in Ahmady *et al.*, this state is identified as a tetraquark [56]. The resulting mass is $M_{\mathrm{AMKMS}} = 1.39$ GeV.

The pion wave functions of the LMZV/BLFQ$_0$ model are similar to those adopted by Gutsche *et al.* [25]. The pion mass is exactly two times the result of Gutsche *et al.* The difference is caused by the presence of the confining interaction in LMZV/BLFQ$_0$ model, which contributes to the other half of the pion mass.

Figure 3 compares the mass spectra of unflavored light mesons and kaons as predicted by LFH with IMA [13], LFH with the power-law like wave function by Gutsche *et al.* [25], LFH with LMZV/BLFQ$_0$ [18], and LFH with 't Hooft potential by Ahmady *et al.* [21]. Overall, LMZV/BLFQ$_0$ provides significant improvement of LFH with IMA towards the experimental data.

In the NR limit, rotational symmetry requires that the combination of the transverse and longitudinal confining interactions is a rotational invariant. The transverse confinement reduces to a harmonic oscillator potential in this limit $\kappa^4\zeta_\perp^2 \to (\kappa^4/4)\vec{r}_\perp^2$. It is expected that the longitudinal confinement also reduces to the quadratic form. The Glazek-Trawinski (GT) model satisfies rotational symmetry in the NR limit by construction. The LMZV model also satisfies this symmetry with the identification $\sigma = \kappa^2/(m_q + m_{\bar{q}})$ in the NR limit. It is curious to note that heavy quark effective theory requires $\kappa \propto \sqrt{M_H} \approx \sqrt{m_q + m_{\bar{q}}}$. Hence, the confining strength σ approaches to a constant in the heavy quark limit. From the fits to the physical quark masses, $\sigma_{\mathrm{HQ}} \approx 0.24$ GeV, where "HQ" stands for "heavy quark" [19]. Physically, this value is determined by the gluon condensate $\langle G_{\mu\nu}G^{\mu\nu}\rangle$, which is in general different from the values in the light sector $\sigma = \langle \bar{q}q\rangle/f_\pi^2 \approx 0.6$ GeV determined by the quark condensate [19].

In coordinate space, the 't Hooft interaction is (recall $\tilde{z} = \frac{1}{2}P^+x^-$)

$$V_{\mathrm{tH}} = g^2|\tilde{z}|. \tag{29}$$

In the NR limit, $\tilde{z} \to -2Mr_z$. The rotational symmetry is not restored with the quadratic transverse confinement from LFH. Note that in Ref. [21], Ahmady *et al.* argued that

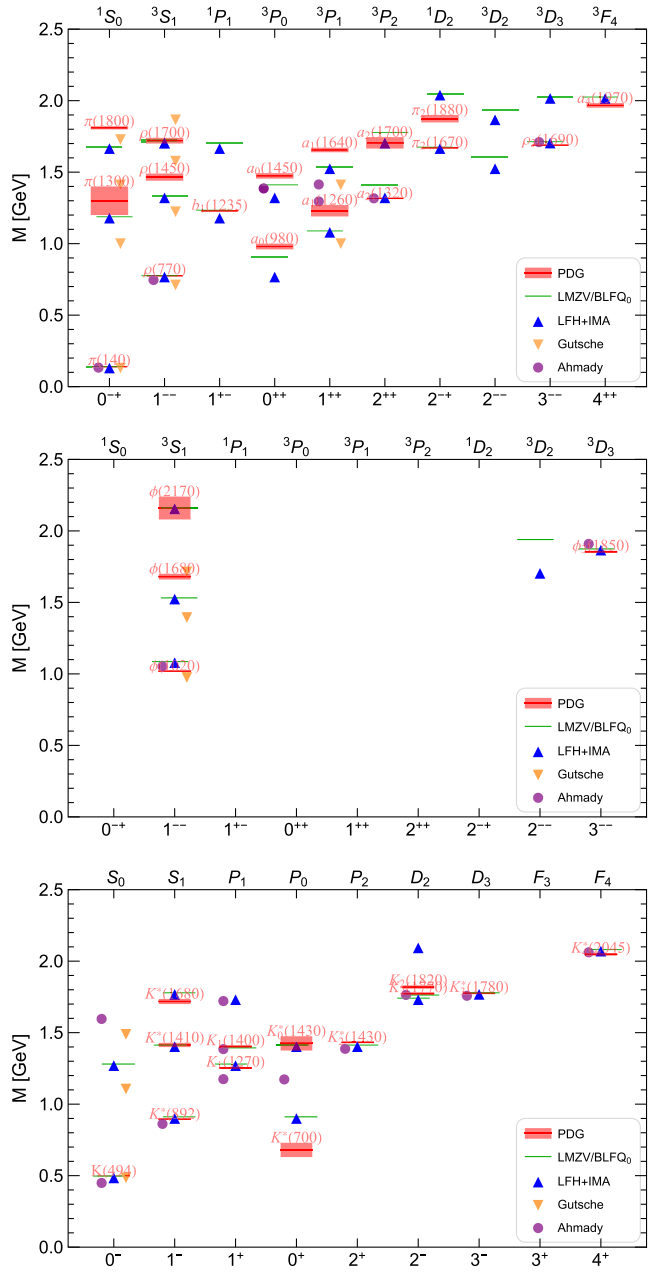

FIG. 3. Comparison of unflavored light meson spectra and kaons as predicted by LFH with IMA [13], with LMZV/BLFQ$_0$ [18] and with 't Hooft potential as implemented by Ahmady *et al.* [21]. Results from Gutsche *et al.* which adopt LFH with a longitudinal wave function similar to LMZV are also attached for comparison [25].

rotational symmetry can be restored with the matching $g = \kappa$, as the transverse LFH confinement and the 't Hooft interaction are equivalent to the c.m., instant form potential $V_\perp = (\kappa^2/2)r_\perp$ and $V_\parallel = (g^2/2)r_z$, respectively, based on an relation $U_{\mathrm{LF}} = V_{\mathrm{IF}} + 2(m_q + m_{\bar{q}})V_{\mathrm{IF}}$ proposed by Trawiński *et al.* [16]. Even if this relation is held in the NR limit, the corresponding potential

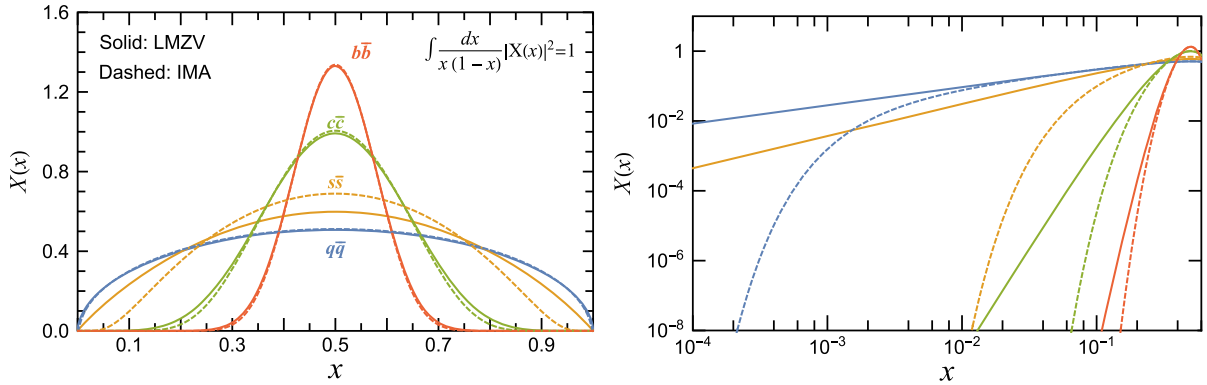

FIG. 4. Comparison of the longitudinal wave functions of ground states from the IMA and from the LMZV model.

$V = V_\perp + V_\parallel = (\kappa^2/2)\left(\sqrt{r_x^2 + r_y^2} + r_z\right)$ is still not rotationally invariant. Shuryak and Zahed proposed an alternative confining interaction that generalizes the 't Hooft model to $3+1$D while combining the light-front holographic interaction [22,23].

$$V_{\rm SZ} = 2\sigma_T\sqrt{\tilde{z}^2 + M^2 r_\perp^2}. \tag{30}$$

The rotational symmetry is restored in the NR limit in this model.

Figure 4 compares the ground-state longitudinal wave functions $X(x) = \sqrt{x(1-x)}\chi(x)$ from the IMA and from the LMZV model. The parameters of the IMA are adopted from LFHQCD [5,13]. For $q\bar{q}$ and $s\bar{s}$, the parameters of the LMZV model are adopted from Ref. [18]. For $c\bar{c}, b\bar{b}$, the parameters are matched to the IMA parameters with the NR reduction, $\sigma = \kappa^2/(m_q + m_{\bar{q}})$. As we can see, the main difference between these two confining potentials is the endpoint asymptotics. Despite the striking similarities of the longitudinal wave functions from IMA and the LMZV model shown in Fig. 4, we would like to emphasize that the endpoint behaviors are dramatically different and this fact has important physical consequences. In the 't Hooft and LMZV models, the endpoint asymptotics is a direct consequence of chiral symmetry breaking and the exponent is related to the chiral condensate. The endpoint behavior also has a dramatic impact on hadronic observables in high energy collisions as hard kernels T_H are sensitive to the endpoint singularities [40].

As an example, one may consider the pion form factor [18]. In light-front holography, the pion form factor is [8,13]

$$F_\pi(Q^2) = \int_0^1 \frac{{\rm d}x}{x(1-x)}|X(x)|^2 \exp\left(-\frac{1-x}{x}\frac{Q^2}{4\kappa^2}\right). \tag{31}$$

The large Q^2 behavior of $F_\pi(Q^2) \sim 1/Q^{1+2\delta}$ is directly related to the endpoint asymptotics of the (normalized) distribution amplitude $X \sim (1-x)^\delta$ [40]. In 't Hooft and LMZV models, $\delta = 1/2 + m_q/\sigma$. Hence, $Q^2 F_\pi(Q^2) \sim 1/\log Q^2$ in the vicinity of the chiral limit. This is in contrast to the LFH prediction $Q^2 F_\pi(Q^2) \to$ const. [8] and to the prediction from LFH with IMA, $Q^2 F_\pi(Q^2) \to e^{-cQ^2}$. These results are shown in Fig. 5, where we adopt parameters from the original LFH [8]. Of course, a comprehensive investigation of the pion form factor in holography requires the dressed holographic current [13], which is beyond the scope of the present work. We only point out that the confined current has similar dependence on the endpoint behavior with the bare current at large Q^2 [58].

A similar example is the pion radiative transition form factor[1] [58,59],

$$Q^2 F_{\pi\gamma}(Q^2) = \frac{4}{\sqrt{3}}\int_0^1 {\rm d}x \frac{\phi_\pi(x,\tilde{Q})}{1-x}, \quad (\tilde{Q} = (1-x)Q). \tag{32}$$

Its value at large Q^2 is predicted to approach different asymptotic values with different asymptotics at the endpoints.

IV. STURM-LIOUVILLE THEORY

After a comparison of various models, a natural question to ask is whether there is freedom for further proposals. This task is not as easy as it seems. Because the construction of a valid Hermitian operator in the functional space may be jeopardized by the singularities in the light-front kinetic energy term. Weller and Miller unified the previous longitudinal potentials with Miller and Brodsky's spatial coordinate $\tilde{z}$ [26]. An alternative approach is the momentum representation,

$$(V_{\rm F}\circ\chi)(x) = \int_0^1 {\rm d}y K(x,y)\chi(y). \tag{33}$$

[1]Here we have neglected the evolution of the pion distribution amplitude since the evolution is extremely slow for large but finite Q^2, say 1 GeV$^2 \lesssim Q^2 \lesssim$ 1000 GeV^2.

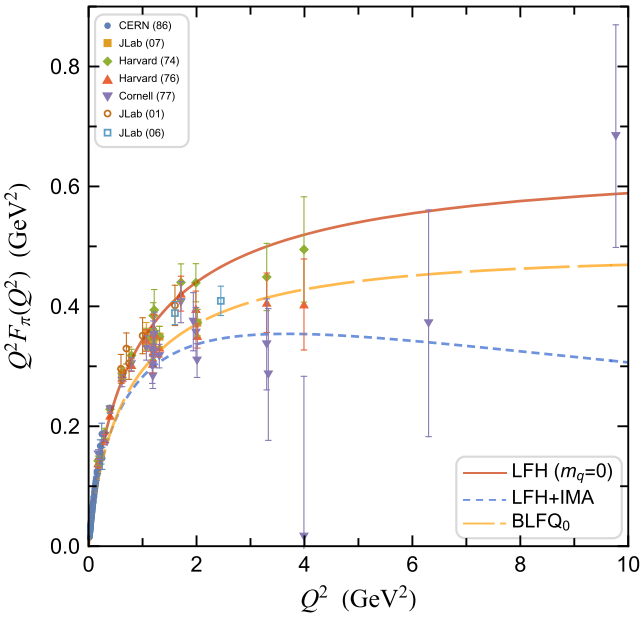

FIG. 5. Large-Q^2 asymptotics of the pion form factor $Q^2F_\pi(Q^2)$ from LFH (solid), LFH with IMA (dotted), and LMZV/BLFQ$_0$ (dashed), for the original parameters of LFH with $\kappa = 0.375$ GeV. The quark masses are $m_{\{u,d\}} = 50$ MeV for LFH with IMA and $m_{\{u,d\}} = 12$ MeV for LMZV/BLFQ$_0$.

The kernel $K(x, y)$ may be related to the coordinate space ($\tilde{z}$) potential,

$$K(x - x') = \int \mathrm{d}\tilde{z} e^{ix\tilde{z}} V_{\parallel}(\tilde{z}). \tag{34}$$

The 't Hooft model $K(x - x') \propto 1/(x - x')^2$ corresponds to the linear potential $V_{\mathrm{tH}} = |\tilde{z}|$, as mentioned. In general, the power-law potential $|\tilde{z}|^p$ leads to a kernel $K(x - x') = \frac{1}{|x-x'|^{p+1}}$ ($p \notin 2\mathbb{N}$). The kernel for the quadratic potential $\tilde{z}^2$ is the derivative of a Dirac δ, which is more convenient to be expressed as differential operators. Due to the low dimensionality, these constructions may be associated with severe singularities.

Another useful tool is the Sturm-Liouville theory. The corresponding interaction takes the form,

$$V_{\mathrm{SL}} = -\partial_x p(x) \partial_x + s(x). \tag{35}$$

Clearly, the LMZV interaction belongs to this category. The longitudinal Schrödinger equation (9) becomes

$$\left[\frac{m_q^2}{x} + \frac{m_{\bar{q}}^2}{1-x} + V_{\mathrm{SL}}\right]\chi(x) = M_{\parallel}^2 \chi(x). \tag{36}$$

It may be written as a Sturm-Liouville problem

$$-(p(x)\chi'(x))' + q(x)\chi(x) = \lambda\chi(x), \qquad (\chi(0) = \chi(1) = 0) \tag{37}$$

where $q(x) = m_q^2/x + m_{\bar{q}}^2/(1-x) + s(x)$. Note that the derivative ∂_x is taken with respect to $\vec{\zeta}_\perp$ not $\vec{r}_\perp$, viz. $\partial_x = (\partial/\partial x)_{\vec{\zeta}_\perp}$. In the NR limit, rotational symmetry can be restored if $p(x = \hat{m}_q) = \kappa^4/[4(m_q + m_{\bar{q}})^2]$.

We shall call this class of potentials as the SL-type, since the longitudinal LFSWE forms a Sturm-Liouville eigenvalue problem (SLEVP). The SL longitudinal confinement is naturally compatible with the transverse holographic confinement in the NR limit. The advantage of these extensions is that the known properties of the SLEVP, e.g., the distribution of eigenvalues can be applied to the longitudinal LFSWE.

To the first approximation, function $p(x)$, stemming from the interquark potential, should be symmetric with respect to the interchange $x \leftrightarrow 1 - x$. Therefore, it can be written as a function of $x(1-x)$ and $(x - \frac{1}{2})^2$. Unless the quark masses are equal, $(x - \frac{1}{2})^2$ is not consistent with the NR reduction $x \approx \hat{m}_q$ and $x \approx \hat{m}_{\bar{q}}$. Therefore, the natural choice of $p(x)$ is $p(x) = \sigma^2[x(1-x)]^\gamma$. A typical source of $s(x)$ is the self-energy correction. A dynamically generated mass may have the asymptotics $\sim B/x(1-x)$, which can be absorbed into the quark mass. In general, we can assume that $s(x)$ is no more singular than the light-front kinetic energy. A convenient choice is $s(x) = 0$.

A comment on the normalization is in order. If, instead, the following normalization is adopted,

$$\int_0^1 \frac{\mathrm{d}x}{x(1-x)} |X(x)|^2 = 1, \tag{38}$$

where a nontrivial weight function $w(x) = 1/[x(1-x)]$ is introduced, the Sturm-Liouville problem for $X(x)$ should be

$$-(P(x)X'(x))' + Q(x)X(x) = \lambda w(x)X(x), \qquad (X(0) = X(1) = 0) \tag{39}$$

where

$$P(x) = p(x)w(x) = \frac{p(x)}{x(1-x)}, \tag{40}$$

$$Q(x) = q(x)w(x) - \frac{pw'^2}{4w} + \frac{1}{2}(pw')' = \frac{q(x)}{x(1-x)} - \frac{8x^2 - 8x + 3}{4x^3(1-x)^3}p(x) + \frac{2x-1}{2x^2(1-x)^2}p'(x). \tag{41}$$

For example, the corresponding interaction for the LMZV model reads

$$U_{\parallel} = -\sigma^2\partial_x^2 + \frac{\sigma^2}{4x^2(1-x)^2}. \tag{42}$$

Now let us turn to the general properties of the SLEVP, which is covered by the Sturm-Liouville theorem [60,61]. The SL problem (37) is called singular if either $p(x) = 0$ at the endpoints or $q(x)$ has singularities. Otherwise, the SL problem is called regular. Clearly, the light-front kinetic energy term in $q(x)$ leads to a singular SLEVP. We remind that the Sturm-Liouville theorem is only applicable to the regular SLEVP or the singular SLEVP in limit circle nonoscillation (LCNO) [60,61]. For other singular SLEVPs, including the limit-circle-oscillation case and the limit-point cases, the properties of the eigenvalues and eigenfunctions are not known in general. For example, the eigenvalues may not be bounded from below; the eigensolutions may have infinite oscillations near the endpoints. Such pathological solutions are known in finite truncations of relativistic bound-state equations, such as the Bethe-Salpeter equations. What is worse is that the classification of singular SLEVP generally relies on the solution. Mathematically, only a finite number of cases are classified. A catalog of the singular SLEVP is given by Ref. [62].

In fact, the most famous SLEVP of the LCNO case on the finite interval [0, 1], is the familiar Legendre function, corresponding to $p(x) = x(1-x)$ and $q(x) = 0$. Here, we have applied a shift $x = (t+1)/2$. The eigenvalues $\lambda_\ell = \ell(\ell+1)$ and the eigenfunctions are the Legendre polynomials $P_\ell(2x-1)$. The longitudinal confinement $V_{\parallel} = -\sigma^2\partial_x(x(1-x)\partial_x)$ covers a number of well-known special functions, the Legendre function, the Chebyshev function and the Gegenbauer function. The most general case is the Jacobi function which is applicable to the general unequal quark mass case,

$$\left[\frac{m_q^2}{x} + \frac{m_{\bar{q}}^2}{1-x} - \sigma^2\frac{\mathrm{d}}{\mathrm{d}x}x(1-x)\frac{\mathrm{d}}{\mathrm{d}x}\right]\chi(x) = M_{\parallel}^2\chi(x). \tag{43}$$

The associated SL problem is

$$-(x(1-x)\chi')' + \left(\frac{\beta^2}{4x} + \frac{\alpha^2}{4(1-x)}\right)\chi = \lambda\chi, \qquad (\chi(0) = \chi(1) = 0) \tag{44}$$

where $\alpha = 2m_{\bar{q}}/\sigma, \beta = 2m_q/\sigma$. The solution are the Jacobi polynomials

$$\chi_n(x) = N_n x^{\frac{\beta}{2}}(1-x)^{\frac{\alpha}{2}}P_n^{(\alpha,\beta)}(2x-1). \tag{45}$$

The eigenvalues are $\lambda_n = (n+\alpha+\beta)(n+1+\alpha+\beta) \propto n^2$. The mass eigenvalue $M_{\parallel n}^2 = (m_q+m_{\bar{q}})^2 + \sigma(m_q+m_{\bar{q}})(2n+1) + \sigma^2 n(n+1)$. The ground state mass obeys the GMOR relation, $M^2 = (m_q+m_{\bar{q}})^2 + \sigma(m_q+m_{\bar{q}})$. The ground state wave function is power-lawlike.

The Jacobi function belongs to an even broader class of special functions, the hypergeometric function [63,64]. It is expected that a broader class of longitudinal confining potentials may be constructed there with hypergeometric functions as the solutions. Unfortunately, the classification of the general hypergeometric differential equation on the interval $[-1, 1]$ is not known.

A similar situation occurs for another large class of second order differential equations on [0, 1], the Heun equation [62,65]. There are at least two special cases of the Heun equation that are related to the LMZV interaction. The first one stems from the azimuthal part of the three-body Schrödinger equation that describes the hydrogen-molecule ion H_2^+ (two protons plus one electron) [65]. It corresponds to a longitudinal potential $V_{\parallel} = -\sigma^2[\partial_x(x(1-x)\partial_x) + \eta(2x-1)^2]$. The eigensolutions are shown to acquire additional exponential factors; $\exp(\pm c|2x-1|)$ [66]. The second case is the Teukolsky equation that describes the stability of the Kerr black hole. It corresponds to a longitudinal potential $V_{\parallel} = -\sigma^2[\partial_x(x(1-x)\partial_x) + a^2(2x-1)^2 + 4a(2x-1)]$ and a mass function $M = m + b(2x-1)$ [65]. The mass correction can also be absorbed into the potential.

The scaling of the eigenvalues is given by the Atkinson-Mingarelli theorem [67]. For large n, λ_n scales quadratically,

$$\lambda_n \sim \frac{n^2\pi^2}{\left(\int_a^b \frac{1}{\sqrt{p(x)}}\right)^2}. \tag{46}$$

From this theorem, the eigenvalues of the SL confining potentials are generally quadratic, unless the integral in the denominator diverges.

A natural generalization of the LMZV model is to consider $p(x) = \sigma^2 x^\gamma(1-x)^\gamma$. Except for $\gamma = 1$, the obtained SLEVPs are not well studied in mathematics. However, as we will see, at least some of these problems (e.g., $\gamma = 0$) are physically well defined. We will investigate the longitudinal potentials with $\gamma = 0, 1, 2, 3$. The results are summarized in Table I. Note that for $\gamma \geq 2, \gamma \in \mathbb{Z}$, the estimate Eq. (46) is not applicable and other distributions of the eigenvalues are possible.

A. Case I: $p(x) = \sigma^2$

In the first case, we take $p(x) = \sigma^2, s(x) = 0$. This is in fact one of the simplest cases. The longitudinal confining potential $V_{\parallel} = \sigma^2\tilde{z}^2$ is quadratic in the longitudinal coordinate space. Then the longitudinal LFSWE becomes

$$\left[\frac{m_q^2}{x} + \frac{m_{\bar{q}}^2}{1-x} - \sigma^2\frac{\mathrm{d}^2}{\mathrm{d}x^2}\right]\chi(x) = M_{\parallel}^2\chi(x). \tag{47}$$

TABLE I. Summary of several longitudinal interactions discussed in this work.

Interaction	$\tilde{z}$-space	$M^2_{\rm gs}$	M^2_n	$\chi(x)$
$-\sigma^2\partial_x^2$	$\sigma^2\tilde{z}^2$		$\sim n^2$	$\sim x(1-x)$
$-\sigma^2\partial_x x(1-x)\partial_x$		$(m_q+m_{\bar{q}})^2+\sigma(m_q+m_{\bar{q}})$	$\sim n^2$	$\sim x^{\frac{m_q}{\sigma}}(1-x)^{\frac{m_{\bar{q}}}{\sigma}}$
$-\sigma^2\partial_x x^2(1-x)^2\partial_x$			$\sim n^2$	$\sim \exp\left(-\frac{2}{\sigma}\sqrt{\frac{m_q^2}{x}+\frac{m_{\bar{q}}^2}{1-x}}\right)$
$-\sigma^2\partial_x x^3(1-x)^3\partial_x$			$\sim n$	$\sim \exp(-\frac{1}{\sigma}(\frac{m_q}{x}+\frac{m_{\bar{q}}}{1-x}))$
$-g^2\frac{1}{(x-x')^2}$	$g^2\lvert\tilde{z}\rvert$	$\sqrt{\frac{\pi}{3}}g(m_q+m_{\bar{q}})$	$\sim n$	$\sim x^{\beta}(1-x)^{\beta'}$

The associated Sturm-Liouville problem, for the equal mass case $m_q = m_{\bar{q}}$, is

$$-\chi''(x)+\frac{\mu^2}{x(1-x)}\chi(x)=\lambda\chi(x), \quad (\chi(0)=\chi(1)=0) \tag{48}$$

where $\mu = m_q/\sigma$, and $\lambda = M^2/\sigma^2$.

This is a 1D Schrödinger equation with a potential $V \propto 1/(x(1-x))$. In the chiral limit ($\mu = 0$), the potential well becomes an infinite square potential well. The solution in this case is the trigonometry function $\chi_n(x) = \sqrt{2}\sin n\pi x$, and the n-th eigenvalue $\lambda_n = n^2\pi^2$, $(n = 1, 2, \ldots)$.[2] The ground-state energy is the zero-point energy, $M^2 = \sigma^2\pi^2$.

For $m_q > 0$, no analytic solution is known so far, although in special cases, the solution is related to the (regularized) hypergeometric function ${}_2F_1$ [63,64]. Numerical solutions are shown in Fig. 6. The nth eigenvalue, again, scales as $\lambda_n \propto n^2$. At the endpoints $x \to 0$, the wave function $\chi(x) \sim x$. Since there is no singularity in the integral of the kinetic energy, the quark mass contribution can be estimated as, $\Delta M^2 = [\gamma_{\rm E} + \ln 2\pi - {\rm Ci}(2\pi)]m_q^2 + O(m_q^4)$, where, $\gamma_{\rm E}$ is Euler's constant, ${\rm Ci}(2\pi) \approx -0.0225607$ is the cosine integral. [63,64].

B. Case II: $p(x) = \sigma^2 x(1-x)$

This case is the LMZV model discussed above.

C. Case III: $p(x) = \sigma^2 x^2(1-x)^2$

In this case, we choose $p(x) = \sigma^2 x^2(1-x)^2$. Then the longitudinal LFSWE becomes

$$\left[\frac{m_q^2}{x}+\frac{m_{\bar{q}}^2}{1-x}-\sigma^2\frac{\rm d}{{\rm d}x}x^2(1-x)^2\frac{\rm d}{{\rm d}x}\right]\chi(x) = M_{\parallel}^2\chi(x). \tag{49}$$

The associated SL problem is

$$-(x^2(1-x)^2\chi')' + \left(\frac{\beta^2}{4x}+\frac{\alpha^2}{4(1-x)}\right)\chi = \lambda\chi, \quad (\chi(0)=\chi(1)=0). \tag{50}$$

The analytical solutions are not known. By matching to the singularities, it can be shown that at the endpoints, the wave functions scales as $\chi(x) \sim \exp[-\frac{2}{\sigma}(\frac{m_q}{\sqrt{x}}+\frac{m_{\bar{q}}}{\sqrt{1-x}})]$. Numerical solutions show the eigenvalues $\lambda_n \propto n$ for low n and $\lambda_n \propto n^2$ for large n.

D. Case IV: $p(x) = \sigma^2 x^3(1-x)^3$

In this case, we choose $p(x) = \sigma^2 x^3(1-x)^3$. Then the longitudinal LFSWE becomes

$$\left[\frac{m_q^2}{x}+\frac{m_{\bar{q}}^2}{1-x}-\sigma^2\frac{\rm d}{{\rm d}x}x^3(1-x)^3\frac{\rm d}{{\rm d}x}\right]\chi(x) = M_{\parallel}^2\chi(x). \tag{51}$$

The associated SL problem is

$$-(x^3(1-x)^3\chi')' + \left(\frac{\beta^2}{4x}+\frac{\alpha^2}{4(1-x)}\right)\chi = \lambda\chi, \quad (\chi(0)=\chi(1)=0). \tag{52}$$

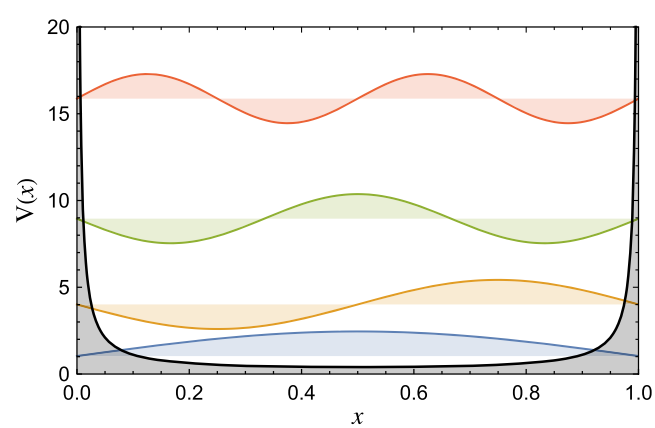

FIG. 6. Solutions of the SL problem (48).

[2]The massless solution $\lambda = 0, \chi(x) = a + bx$, is eliminated by the boundary condition.

The analytical solutions are not known. By matching to the singularities, it can be shown that at the endpoints, the wave functions scale as $\chi(x) \sim \exp[-\frac{1}{\sigma}(\frac{m_q}{x} + \frac{m_{\bar{q}}}{1-x})]$. Numerical calculations show that the eigenvalues $\lambda_n \propto n$.

This case is closely related to the Głazek-Trawiński potential introduced above. To see this, we can express the longitudinal coordinate $\zeta_\parallel = i\nabla_{\kappa_\parallel}$ of Głazek and Trawiński in terms of $\tilde{z} = i\partial_x$. Recall, in the equal mass case, $\kappa_\parallel = m_q \frac{2x-1}{\sqrt{x(1-x)}}$, or equivalently, $x = (1/2)\left(1 + \kappa_\parallel / \sqrt{4m_q^2 + \kappa_\parallel^2}\right)$. Then, we can obtain $\zeta_\parallel = (2/m_q)\sqrt{x^3(1-x)^3} i\partial_x$. Therefore, the longitudinal confinement in this model becomes

$$V_\parallel^{(\mathrm{GT})} = -\frac{4\lambda^2}{m_q^2}\partial_x x^3(1-x)^3\partial_x. \tag{53}$$

The confining strength $\sigma = \frac{2\lambda}{m_q}$. With this identification, the wave function at the endpoints becomes, $\chi(x) \sim \exp(-\frac{m_q^2}{2\lambda x(1-x)})$, in agreement with Głazek and Trawiński's wave function.

There is a caveat here since $\kappa_\perp = \vec{k}_\perp / \sqrt{x(1-x)}$ contains the longitudinal coordinate x. Therefore, $\vec{k}_\perp = \vec{\kappa}_\perp / \sqrt{4 + \kappa_\parallel^2/m_q^2}$ also depending on $\kappa_\parallel$. To obtain the third coordinate $\zeta_\parallel$, we can apply the chain rule,

$$\zeta_\parallel \equiv i\frac{\partial}{\partial \kappa_\parallel} \tag{54}$$

$$= \frac{\partial \vec{k}_\perp}{\partial \kappa_\parallel} \cdot \vec{r}_\perp + \frac{\partial x}{\partial \kappa_\parallel} P^+ r_+ \tag{55}$$

$$= -\frac{1}{2}\left(x - \frac{1}{2}\right) x^{\frac{1}{2}}(1-x)^{\frac{1}{2}} m_q^{-1} \vec{k}_\perp \cdot \vec{r}_\perp + 2x^{\frac{3}{2}}(1-x)^{\frac{3}{2}} m_q^{-1} \tilde{z}. \tag{56}$$

Here $\vec{r}_\perp = i\partial/\partial\vec{k}_\perp$, $r_+ = i\partial/\partial k^+$, and $P^+ r_+ \equiv \tilde{z} = i\partial_x$ is Brodsky and Miller's frame-independent longitudinal coordinate. Since $\partial\vec{k}_\perp/\partial\kappa_\parallel \neq 0$, in general $\zeta_\parallel$ depends on $\vec{r}_\perp$. In other words, $\vec{\kappa}$ and $\vec{\zeta}$ are not independent conjugate pairs, and the longitudinal interaction constructed here may not be exactly the same as the Głazek-Trawiński model.

V. SUMMARY AND OUTLOOKS

In this work, we discussed the role of longitudinal dynamics in semi-classical light-front Schrödinger wave equations. Based on a separation of variables ansatz, we relate the longitudinal confining interaction to the endpoint asymptotics of the resulting wave function as well as to the scaling of the eigenvalues. This enables us to compare longitudinal interactions proposed in the recent literature as well as a broader class of longitudinal interactions based on the Sturm-Liouville theory. We analyzed several concrete cases $V_\parallel \sim -\partial_x x^\gamma (1-x)^\gamma \partial_x$ ($\gamma = 0, 1, 2, 3$). We also pointed out the challenges for constructing valid longitudinal interactions due to the presence of the endpoint singularities in the light-front kinetic energy.

Our motivation is to search for a plausible first approximation to mesons in conjunction with light-front holography. Both the 't Hooft interaction $\propto |\tilde{z}|$ and the LMZV interaction $\propto \partial_x(x(1-x))\partial_x$ implement the chiral symmetry breaking for the pion. They both produce power-lawlike wave functions at the endpoints. On the other hand, interactions of quadratic form naturally match the transverse holographic confining potential in the nonrelativistic limit. We further expect that the resulting wave functions can be used as a basis for the full quantum many-body calculations. In this regard, the LMZV interaction is useful for its computational convenience. Indeed, the longitudinal wave functions from this interaction, the power-law weighted Jacobi polynomials, form a standard basis for wave functions with power-law behavior, such as the solution of the 't Hooft model. Other longitudinal interactions may be useful in different contexts.

We focused on the light mesons. The reason is that the hyperfine structure of the heavy systems, including the heavy-light mesons are dominated by the one-gluon-exchange interaction [17,28]. A single confining interaction is not sufficient. Indeed, the works on heavy systems have to introduce additional parameters. Moreover, the restoration of the 3D rotational symmetry in the nonrelativistic limit puts strong constraints on the confining interactions.[3] As such, different forms of the longitudinal confinement become nearly identical.

One of the interesting questions is how to generalize the present investigation to the multiparton sectors, including notably the baryons. There have been several proposals in the literature, including the pairwise longitudinal interactions [68,69], the quark-diquark model [21,70], and the orthogonal basis over a k-simplex (triangle, tetrahedron,...) [24,71–73].

ACKNOWLEDGMENTS

We wish to thank S. J. Brodsky and G. F. de Téramond for enlightening discussions and for their critical reading of an earlier version of the manuscript. We also gratefully acknowledge fruitful discussions with S. J. Brodsky, G. F.

[3]Here we only retain those longitudinal confining forms that reduce to the harmonic oscillator in the nonrelativistic limit due to another symmetry constraint: we require factorization of the CM motion from the internal motion.

de Téramond, G. A. Miller, X. Zhao, C. Mondal, J. Hiller, R. Sandapen, S. Kaur, E. Shuryak, I. Zahed, P. Mannheim, S. D. Glazek, and Q. Wang. This work is supported in part by the Department of Energy under Grants No. DE-FG02-87ER40371, and No. DE-SC0018223 (SciD AC4/NUCLEI). Y. L. is supported by the New faculty startup fund of the University of Science and Technology of China.

[1] G. F. de Teramond and S. J. Brodsky, Phys. Rev. Lett. **102**, 081601 (2009).
[2] S. J. Brodsky and G. F. de Teramond, Phys. Rev. Lett. **96**, 201601 (2006).
[3] H. G. Dosch, G. F. de Teramond, and S. J. Brodsky, Phys. Rev. D **92**, 074010 (2015).
[4] H. G. Dosch, G. F. de Teramond, and S. J. Brodsky, Phys. Rev. D **95**, 034016 (2017).
[5] M. Nielsen, S. J. Brodsky, G. F. de Téramond, H. G. Dosch, F. S. Navarra, and L. Zou, Phys. Rev. D **98**, 034002 (2018).
[6] L. Zou, H. G. Dosch, G. F. De Téramond, and S. J. Brodsky, Phys. Rev. D **99**, 114024 (2019).
[7] A. Deur, S. J. Brodsky, and G. F. de Teramond, Nucl. Phys. **90**, 1 (2016).
[8] S. J. Brodsky and G. F. de Teramond, Phys. Rev. D **77**, 056007 (2008).
[9] S. J. Brodsky and G. F. de Teramond, Phys. Rev. D **78**, 025032 (2008).
[10] R. S. Sufian, G. F. de Téramond, S. J. Brodsky, A. Deur, and H. G. Dosch, Phys. Rev. D **95**, 014011 (2017).
[11] G. F. de Teramond, T. Liu, R. S. Sufian, H. G. Dosch, S. J. Brodsky, and A. Deur (HLFHS Collaboration), Phys. Rev. Lett. **120**, 182001 (2018).
[12] T. Liu, R. S. Sufian, G. F. de Téramond, H. G. Dosch, S. J. Brodsky, and A. Deur, Phys. Rev. Lett. **124**, 082003 (2020).
[13] S. J. Brodsky, G. F. de Teramond, H. G. Dosch, and J. Erlich, Phys. Rep. **584**, 1 (2015).
[14] S. S. Chabysheva and J. R. Hiller, Ann. Phys. (Amsterdam) **337**, 143 (2013).
[15] S. D. Glazek and A. P. Trawiński, Phys. Rev. D **88**, 105025 (2013).
[16] A. P. Trawiński, S. D. Głazek, S. J. Brodsky, G. F. de Téramond, and H. G. Dosch, Phys. Rev. D **90**, 074017 (2014).
[17] Y. Li, P. Maris, X. Zhao, and J. P. Vary, Phys. Lett. B **758**, 118 (2016).
[18] Y. Li and J. P. Vary, Phys. Lett. B **825**, 136860 (2022).
[19] G. F. de Téramond and S. J. Brodsky, Phys. Rev. D **104**, 116009 (2021).
[20] M. Ahmady, H. Dahiya, S. Kaur, C. Mondal, R. Sandapen, and N. Sharma, Phys. Lett. B **823**, 136754 (2021).
[21] M. Ahmady, S. Kaur, S. L. MacKay, C. Mondal, and R. Sandapen, Phys. Rev. D **104**, 074013 (2021).
[22] E. Shuryak and I. Zahed, arXiv:2111.01775.
[23] E. Shuryak and I. Zahed, arXiv:2112.15586.
[24] E. Shuryak and I. Zahed, arXiv:2202.00167.
[25] T. Gutsche, V. E. Lyubovitskij, I. Schmidt, and A. Vega, Phys. Rev. D **87**, 056001 (2013).
[26] C. M. Weller and G. A. Miller, Phys. Rev. D **105**, 036009 (2022).
[27] J. P. Vary, H. Honkanen, J. Li, P. Maris, S. J. Brodsky, A. Harindranath, G. F. de Teramond, P. Sternberg, E. G. Ng, and C. Yang, Phys. Rev. C **81**, 035205 (2010).
[28] S. Godfrey and N. Isgur, Phys. Rev. D **32**, 189 (1985).
[29] A. Szczepaniak, E. S. Swanson, C. R. Ji, and S. R. Cotanch, Phys. Rev. Lett. **76**, 2011 (1996).
[30] H. Reinhardt, G. Burgio, D. Campagnari, E. Ebadati, J. Heffner, M. Quandt, P. Vastag, and H. Vogt, Adv. High Energy Phys. **2018**, 2312498 (2018).
[31] S. Okubo, Prog. Theor. Phys. **12**, 603 (1954).
[32] K. Suzuki and S. Y. Lee, Progr. Theor. Phys. **64**, 2091 (1980).
[33] K. Suzuki, Progr. Theor. Phys. **68**, 246 (1982).
[34] K. Suzuki, Progr. Theor. Phys. **68**, 1999 (1982).
[35] K. Suzuki and R. Okamoto, Progr. Theor. Phys. **70**, 439 (1983).
[36] K. Suzuki and R. Okamoto, Progr. Theor. Phys. **92**, 1045 (1994).
[37] S. D. Glazek and K. G. Wilson, Phys. Rev. D **48**, 5863 (1993).
[38] S. D. Glazek and K. G. Wilson, Phys. Rev. D **49**, 4214 (1994).
[39] F. Wegner, Ann. Phys. (N.Y.) **506**, 77 (1994).
[40] G. P. Lepage and S. J. Brodsky, Phys. Rev. D **22**, 2157 (1980).
[41] R. J. Perry, A. Harindranath, and K. G. Wilson, Phys. Rev. Lett. **65**, 2959 (1990).
[42] K. G. Wilson, T. S. Walhout, A. Harindranath, W. M. Zhang, R. J. Perry, and S. D. Glazek, Phys. Rev. D **49**, 6720 (1994).
[43] S. D. Glazek, Acta Phys. Pol. B **43**, 1843 (2012).
[44] S. D. Głazek, M. Gómez-Rocha, J. More, and K. Serafin, Phys. Lett. B **773**, 172 (2017).
[45] K. Serafin, M. Gómez-Rocha, J. More, and S. D. Głazek, Eur. Phys. J. C **78**, 964 (2018).
[46] S. J. Brodsky, S. Gardner, and D. S. Hwang, Phys. Rev. D **73**, 036007 (2006).
[47] S. J. Brodsky, H. C. Pauli, and S. S. Pinsky, Phys. Rep. **301**, 299 (1998).
[48] J. S. Schwinger, Phys. Rev. **128**, 2425 (1962).
[49] G. 't Hooft, Nucl. Phys. **B75**, 461 (1974).
[50] Y. z. Mo and R. J. Perry, J. Comput. Phys. **108**, 159 (1993).
[51] J. Eisert, M. Cramer, and M. B. Plenio, Rev. Mod. Phys. **82**, 277 (2010).
[52] Y. Li, P. Maris, and J. P. Vary, Phys. Rev. D **96**, 016022 (2017).
[53] G. A. Miller and S. J. Brodsky, Phys. Rev. C **102**, 022201 (2020).

[54] S. J. Brodsky and G. F. de Teramond, Subnucl. Ser. **45**, 139 (2009).
[55] M. Gell-Mann, R. J. Oakes, and B. Renner, Phys. Rev. **175**, 2195 (1968).
[56] M. Nielsen and S. J. Brodsky, Phys. Rev. D **97**, 114001 (2018).
[57] X. Ji, Y. Liu, and I. Zahed, Phys. Rev. D **103**, 074002 (2021).
[58] S. J. Brodsky, F. G. Cao, and G. F. de Teramond, Phys. Rev. D **84**, 075012 (2011).
[59] R. Swarnkar and D. Chakrabarti, Phys. Rev. D **92**, 074023 (2015).
[60] A. M. Krall, *Applied Analysis* (D. Reidel Publishing Co., Dordrecht, Holland, 1986).
[61] A. Zettl, *Sturm-Liouville Theory* (American Mathematical Society, 2005).
[62] W. N. Everitt, A catalogue of Sturm-Liouville differential equations, in *Sturm-Liouville Theory: Past and Present*, edited by W. O. Amrein, A. M. Hinz, and D. B. Pearson (Birkhuser Verlag, Basel, 2005), ISBN: 3-7643-7066-1.
[63] *Handbook of Mathematical Functions with Formulas, Graphs, and Mathematical Tables*, edited by M. Abramowitz and I. A. Stegun, 9th reprint with additional corrections of tenth original printing with corrections (Dover, New York, 1983), ISBN 978-0-486-61272-0.
[64] NIST Digital Library of Mathematical Functions, http://dlmf.nist.gov/, Release 1.1.4 of 2021-01-15. F. W. J. Olver, A. B. Olde Daalhuis, D. W. Lozier, B. I. Schneider, R. F. Boisvert, C. W. Clark, B. R. Miller, B. V. Saunders, H. S. Cohl, and M. A. McClain, eds.
[65] S. Yu. Slavyanov and W. Lay, *Special Functions: A Unified Theory Based on Singularities* (Oxford University Press, New York, 2000).
[66] A. V. Mitin, arXiv:1508.01359v2.
[67] F. V. Atkinson and A. B. Mingarelli, J. Reine Angew. Math. (Crelle) **375/376**, 380393 (1987).
[68] C. Mondal, S. Xu, J. Lan, X. Zhao, Y. Li, D. Chakrabarti, and J. P. Vary, Phys. Rev. D **102**, 016008 (2020).
[69] S. Xu, C. Mondal, J. Lan, X. Zhao, Y. Li, and J. P. Vary (BLFQ Collaboration), Phys. Rev. D **104**, 094036 (2021).
[70] A. Yu, https://dr.lib.iastate.edu/handle/20.500.12876/31997.
[71] S. S. Chabysheva, B. Elliott, and J. R. Hiller, Phys. Rev. E **88**, 063307 (2013).
[72] S. S. Chabysheva and J. R. Hiller, Phys. Rev. E **90**, 063310 (2014).
[73] M. Burkardt, S. S. Chabysheva, and J. R. Hiller, Phys. Rev. D **94**, 065006 (2016).